SEACI Project 3.1.3 Milestone Report

Assessment of potential predictability of seasonal climate in SE Australia using the Bureau of Meteorology's dynamical seasonal forecast system

Harry Hendon, Guo Liu, Oscar Alves, Guomin Wang

hhh@bom.gov.au

BMRC, 700 Collins Street, Melbourne, Australia

1. Introduction

The Bureau of Meteorology routinely makes dynamical seasonal predictions out to 9 month lead time with the POAMA coupled ocean-atmosphere forecast system. POAMA (Predictive Ocean Atmosphere Model for Australia) is an intra-seasonal to inter-annual climate prediction system based on coupled ocean and atmosphere general circulation models. The main focus for POAMA-1 is the prediction of sea surface temperature (SST) anomalies associated with El Niño / La Niña, for which POAMA's predictions are internationally competitive. El Niño/Southern Oscillation (ENSO) is the dominant driver of Australian climate variability, thus POAMA's forecasts have great value for anticipating the behavior of El Niño.

The POAMA system is continually evolving and improving, and subsequent versions of POAMA will address problematic bias and drift that hinder direct prediction of regional climate variations, such as rainfall and temperature across continental Australia. New versions of POAMA will have improved horizontal resolution and improved parameterization of physical processes so as to better resolve and simulate regional climate. Future development of the components of the POAMA system will be done as part of the ACCESS project. ACCESS is a joint Bureau, CSIRO, and Australian Universities project that aims at coordinated development of core components of an earth system model and data assimilation systems to support a range of applications, including the POAMA seasonal prediction. These developments should improve the direct prediction of regional climate variability.

However, even assuming model drift and bias can be improved and that increased resolution leads to better regional climate simulation, the degree of predictability of regional climate is unknown.Perfect prediction of the slowly varying surface boundary forcing (primarily tropical sea surface temperatures; SST), which is thought to be the main source of seasonal climate predictability, will predict only a portion of actual climate variability due to the presence of internal atmospheric noise. Nonetheless, an assessment of the theoretical upper limit of predictability, given perfect knowledge of the slowly varying boundary forcing, will provide an upper bound on the expected skill of the POAMA system. This report focuses on the assessment of potential predictability of rainfall and the relative role of boundary forcing from the tropical Pacific and Indian Oceans.

2. Atmospheric Model Component of POAMA-1 and experimental design

The atmospheric component of POAMA-1is based on version 3 of the Bureau’s Atmospheric Model (Colman et al. 2004). The atmospheric model is run with modest horizontal resolution (~300 km resolution) and with 17 vertical levels. The primary deficiencies of this modest atmospheric resolution are the inability to resolve local climate variations associated with regional topography and orography (e.g. the Dividing Range is not well represented) and extratropical storm tracks that are too diffuse.

To assess potential predictability of regional climate, we assume perfect knowledge of the slow variation of tropical SST for the period 1982-2003. Effectively, we replace the ocean model component of POAMA with a prescription of the SST variation that actually occurred. We prescribe these observed variations of SST at latitudes equatorward of 30 degrees. Poleward of 30 degs latitude, climatological SST is prescribed. We refer to this experiment as “global SST”. An ensemble of eight integrations is carried out so as to sample the atmospheric noise that is unrelated to the slow variation of boundary forcing. Initial conditions for each member differ only slightly.

To assess the relative roles of forcing from the Pacific and Indian Oceans, we conduct 3 additional experiments. In “Pacific large”, observed SST variations are prescribed in the entire tropical Pacific Ocean, while climatological SST is prescribed elsewhere. In “Pacific small”, observed SST is prescribed only in the eastern tropical Pacific Ocean. These two experiments are aimed at elucidating the global teleconnections that are driven by SST variations associated with El Niño/Southern Oscillation (ENSO). The Pacific small runs are aimed at understanding the forcing by SST variations in the main El Niño region of the equatorial eastern Pacific. The Pacific large runs include the SST forcing in the far western Pacific, where anomalies during ENSO tend to be out of phase with those in the eastern Pacific. The role of Indian Ocean SST is highlighted in the Indian experiment, where observed SST variations are prescribed only in the tropical Indian Ocean. In all cases, 8 ensemble members are generated for the period 1982-2003 using slightly different initial conditions.

3. Potential Predictability of Rainfall

Analysis of variance (Scheffe 1959) is used to isolate the potentially predictable signal produced by the slow evolution of prescribed SST from the unpredictable atmospheric background noise (e.g., Rowell et al. 1995). Let a seasonal mean (e.g., September-November average) anomaly at a given location be denoted by a_{ik}, where i is the year index that goes from 1 to 22 (years 1982-2003) and k the ensemble number of the AGCM run that goes from 1 to 8. For year i, the predictable climate signal (CS_i) is estimated as the average of all 8 members, that is,

$$CS_i = \frac{1}{8}\sum_{k=1}^{8} a_{ik}$$

The climate noise for run number k and year i (CN_{ik}) is simply the deviation from the predictable signal, that is

$$CN_{ik} = a_{ik} - CS_i.$$

The variance of the unpredictable noise for year i can then be obtained by

$$vn_i = \frac{1}{7}\sum_{k=1}^{8} CN_{ik}^2$$

Note that the denominator is 7 instead of 8 because the degrees of freedom are one less than the total number of realizations for a second moment.

Let VN represent the average of noise variance over all 22 years of simulation;

$$VN = \frac{1}{22}\sum_{i=1}^{22} vn_i$$

Although the monthly mean climatology is already removed from the monthly dataset, we recalculate the yearly mean climatology as

$$CLIM = \frac{1}{22}\sum_{i=1}^{22} CS_i$$

The variance of the climate signal (VS), which is the predictable component of the variability, is simply obtained with reference to CLIM, as

$$VS = \frac{1}{22-1}\sum_{i=1}^{22} (CS_i - CLIM)^2$$

Again, there is one less than the total degrees of freedom for this second moment.

The estimate of the climate signal for a given year is obtained from an ensemble of only 8 members. It represents a small sample estimate. Because of the uncertainty in estimating CS_i from the true population climate signal, VS will always overestimate the externally forced variability. The amount of overestimation is VN/8, according to a standard analysis of variance (e.g., Scheffe 1959). We thus subtract VN/8 from our estimate of VS to obtain a more accurate estimate of the predictable component of climate variability. The total variance then can be represented as Vartot=VS+VN. An estimation of the predictable signal strength is simply the ratio of VS/Vartot. Computation of predictable signal strength is done for each season (DJF, MAM, JJA, and SON) in order to elucidate, for instance, seasonal dependence of predictability stemming from El Niño.

The potentially predictable rainfall, as indicated by the ratio VS/Vartot, is displayed in Fig. 1 for each season (DJF, MAM, JJA, and SON). This analysis indicates that SE Australian rainfall is most predictable (in the BAM3 model) in autumn through spring, when up to 30% of the rainfall variance is predictable. That is, if we could perfectly predict global tropical SST, the maximum amount of rainfall variability that we could expect to predict is about 30%. This estimation of potential predictability is in line with the observed rainfall variance accounted for by El Niño (Fig. 2), which is the dominant source of interannual variation of SST.

Based on our additional experiments, the source of potential predictability can be attributed to the SST variations in the Indian Ocean and/or Pacific Ocean. The motivation for this attribution is both to better understand the source of predictability but to also provide insight into where improvements in the prediction system might lead to the greatest improvement of prediction. Interestingly, a large portion of the predictable rainfall variability in the SE during spring (SON; Fig 3) and winter (JJA; Fig. 4) stems from SST variations in the tropical Indian Ocean. This might appear to be counter to the notion that ENSO is the main driver of rainfall variability during these seasons. However, during ENSO SST anomalies co-vary in the Indian Ocean with those in the equatorial Pacific (Fig. 5). For instance, in the SON season, warm SST anomalies in the central Pacific during El Niño tend to co-occur with cold anomalies in the eastern equatorial Indian Ocean. Thus, it is possible that predictability arising from ENSO stems from the coherent variation of SST in the Indian Ocean and not as a direct result of SST variations in the equatorial Pacific. This is confirmed in Figures 6 and 7, which show the correlations of rainfall with the Nino4 index in each of the four experiments. Figures 6a and 7a are identical to

Figures 2d and c, respectively. That is, they show the correlation of simulated rainfall with the Nino4 SST index for the runs with SST prescribed throughout the global tropics. Inspection of the other panels in Fig. 6 and 7 reveals that a large portion of the rainfall relationship in the SE during ENSO actually stems from the SST forcing in the Indian Ocean that accompanies ENSO.

We provide further insight into the role of SST variations in the two ocean basins by diagnosing the patterns of SST variability that are related to the predictable rainfall anomalies in the SE. We do this by computing the correlation of the ensemble mean rainfall time series averaged over SE Australia (35-40S, 130-140E) with SST at each grid point (over land points we use the model's simulated land surface temperature). For the SON season, the pattern of SST that correlates to SE Australian rainfall for the global experiment (Fig. 8a) is nearly identical to that associated with La Niña (opposite sign of Fig. 5 d). This confirms that SE rainfall is responding strongly to El Niño/La Niña. But, rainfall is nearly equally sensitive to Indian Ocean SST (Fig. 8c) as it is to eastern equatorial Pacific SST (Fig. 8d). However, close inspection of Fig. 8 reveals that the peak correlation with SST in the eastern Pacific for the Pac-small experiment is slightly lower than for the global experiment. This further suggests that the coherent variation of SST during ENSO in the Indian Ocean is an additional source of predictability beyond that of El Niño in the Pacific.

4. Conclusions

Based on analysis of a suite of "perfect SST" experiments with the atmospheric model of the POAMA seasonal forecasts system, SE Australian rainfall is found to be most predictable in autumn through spring, when up to 30% of the rainfall variance is predictable. That is, if we could perfectly predict global sea surface temperatures, the maximum amount of rainfall variability that we could expect to predict is about 30%. This estimate of 30% is an upper limit, as we know that we can never perfectly predict SST. Nonetheless, SST is highly predictable at short lead time. Furthermore, there may be some additional predictability at short lead time as a result of anomalous initial land surface conditions (e.g., soil moisture anomalies) or low frequency atmospheric disturbances (e.g., the MJO). Such a possibility is being explored with new versions of POAMA that have improved land surface and atmospheric initialization. Therefore, 30% predictability should not be viewed as being unattainable. Nonetheless, the potential usefulness of 30% predictability of rainfall needs to be assessed. For instance, predictability of crop yield or stream flow could be assessed based on output from this ensemble of simulations, where both the predictable component and noise component of the climate is known and well sampled.

The estimation of potential predictability of SE Australian rainfall in this study, while highly dependent on the model that was used, is in line with the observed rainfall variance that is accounted for by El Niño, which is the dominant source of interannual variation of SST and of rainfall variability. Interestingly, this study indicates that a large portion of the predictable rainfall variability in the SE during spring and winter stems from SST variations in the tropical Indian Ocean. This might appear to be counter to the notion that ENSO is the main driver of rainfall variability during these seasons. However, during ENSO SST anomalies co-vary in the Indian Ocean with those in the equatorial Pacific, and it is this co-varying SST in the Indian Ocean that drives a significant portion of the predictable rainfall variations in the SE.

These results indicate that improvement of rainfall prediction in the SE from the POAMA system will require improved initialization and simulation of the Indian Ocean. Currently, model bias and lack of accurate initial oceanic and atmospheric conditions hinder the ability to predict the coupled-state of the Indian Ocean. However, improvements to the POAMA component models should alleviate some of the bias in the Indian Ocean (in particular, the overall cold SST bias and elevation of the thermocline in the eastern Indian Ocean). Furthermore, a new ocean assimilation system is nearing completion and will be part of the POAMA 2 system. This new assimilation scheme, which initializes salinity, temperature and currents, shows great promise for improved initialization of the Indian Ocean. Experiments to assess its impact on predictability of Australian climate will commence shortly.

References

Colman, R., L. Deschamps, M. Naughton, L. Rikus, A. Sulaiman, K. Puri, G, Roff, Z. Sun and G. Embery, 2004: BMRC Atmospheric Model (BAM) version 3.0: Comparison with mean climatology, BMRC Research. Report, No. **98** (available from http://www.bom.gov.au/bmrc).

Rowell, D. P., C. K. Folland, K. Maskell, and M. N. Ward, 1995: Variability of summer rainfall over tropical North Africa (1906–92): Observations and modelling. *Quart. J. Roy. Meteor. Soc.,* **121,** 669–704..

Scheffe, H., 1959: *The Analysis of Variance.* John Wiley and Sons, 477 pp..

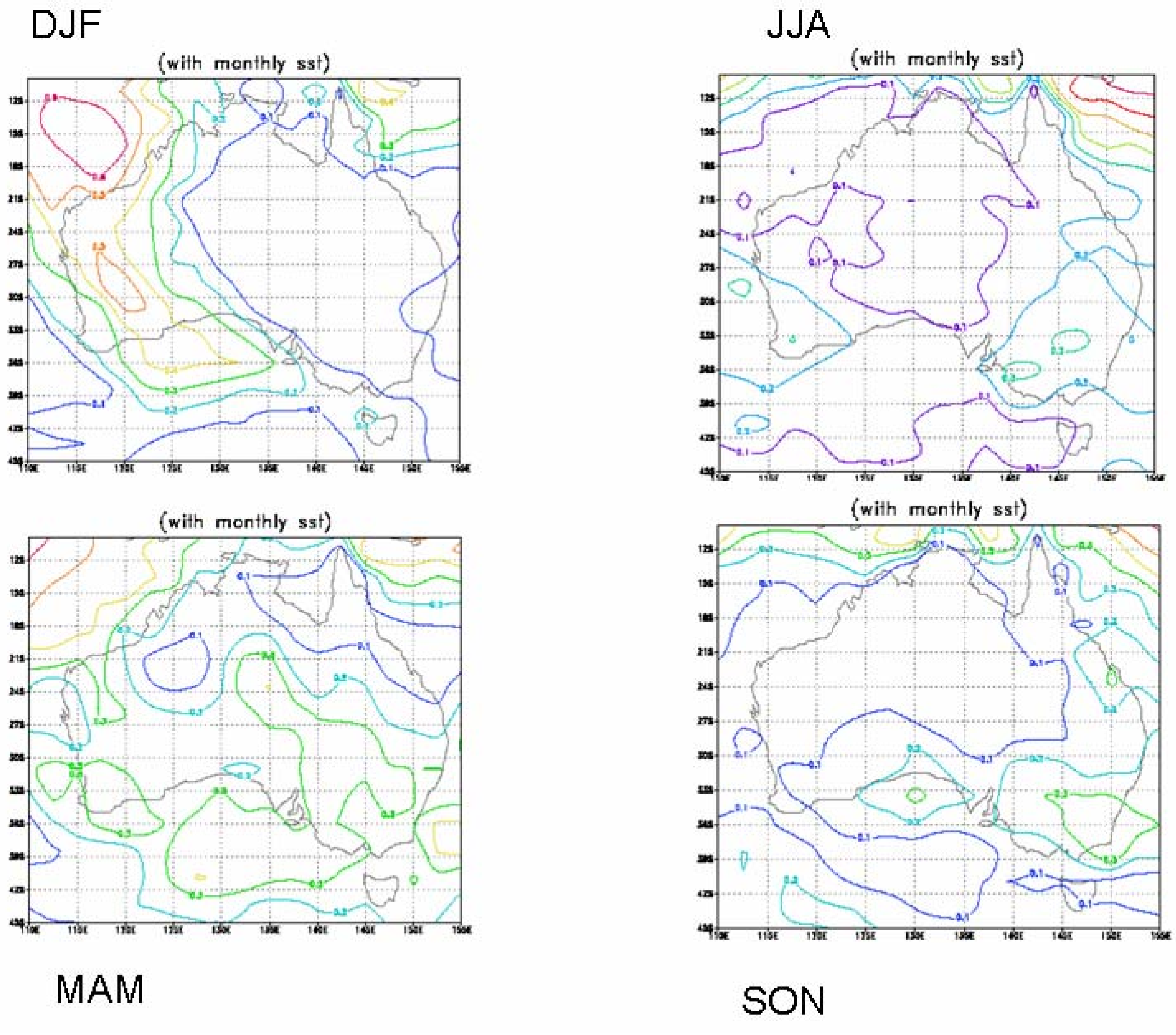

Figure 1. Predictable fraction of rainfall variability forced by global SST for the four seasons

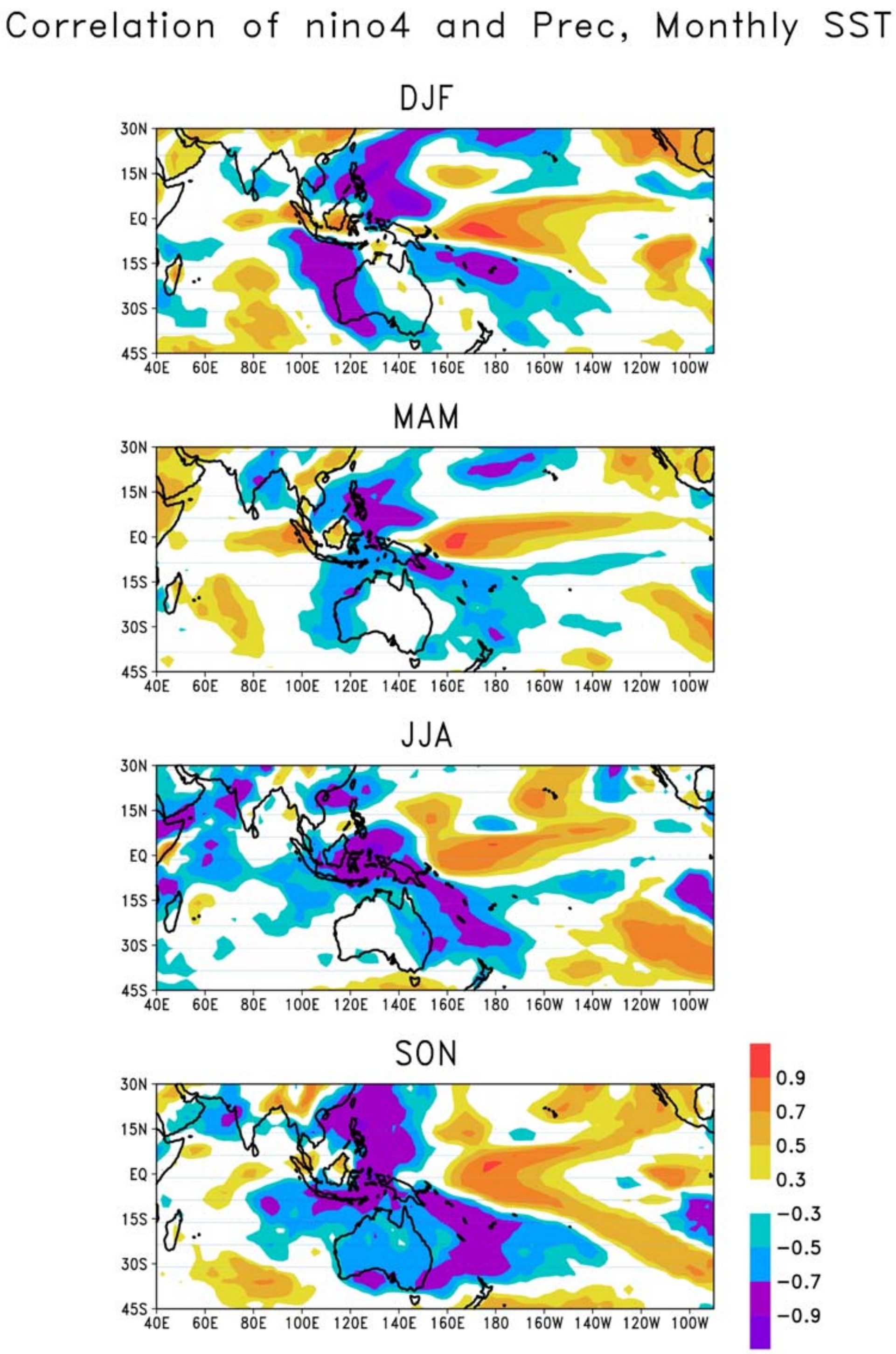

Figure 2. Correlation of simulated rainfall with the Nino4 SST index, by season. Note the correlation in SE Australia in SON ranges up to about 0.6, which implies that about 35% of the rainfall variability is accounted for by El Niño.

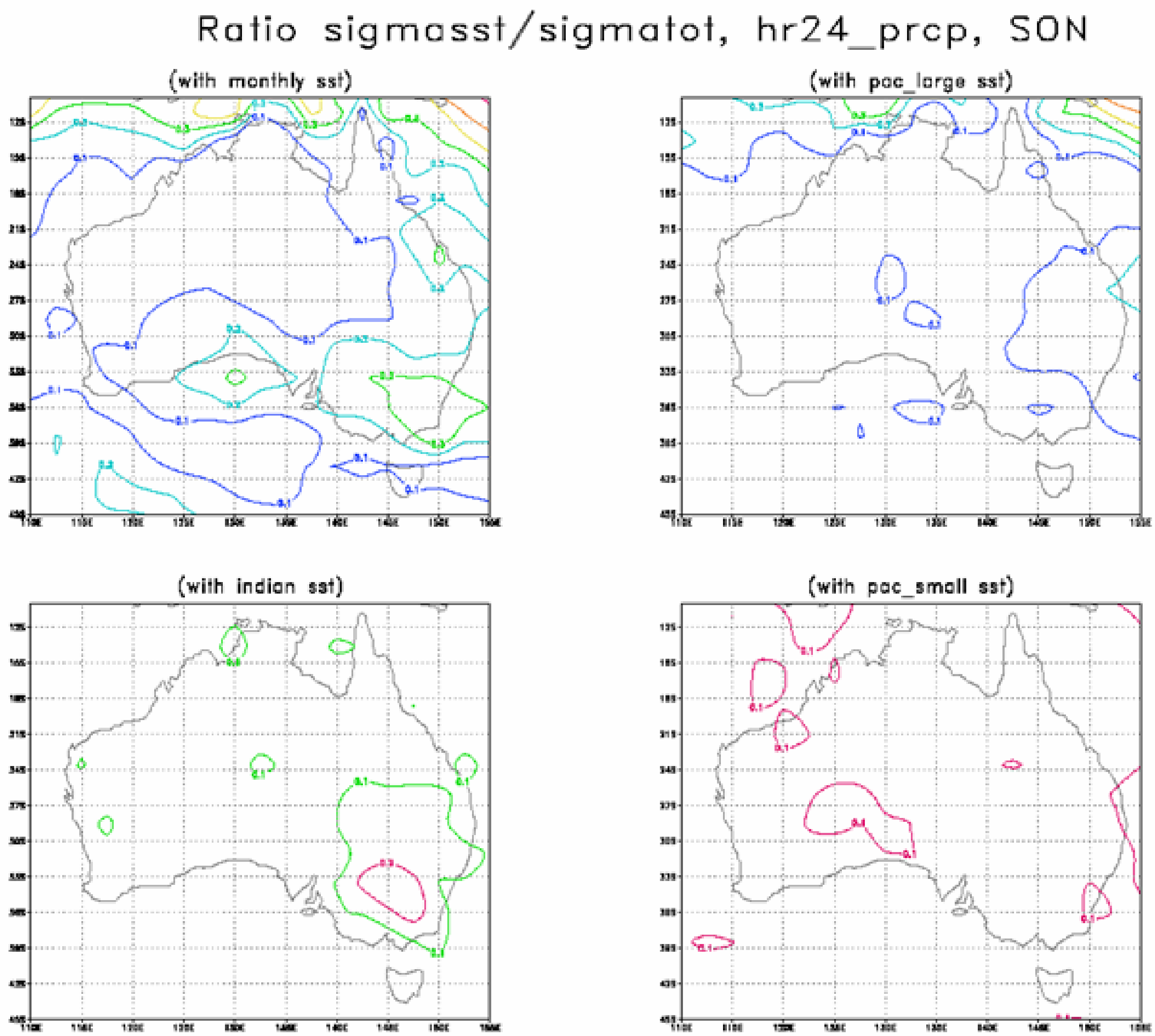

Figure 3. Predictable fraction of spring time rainfall variability forced by a) global SST, b) Indian Ocean SST, c) tropical Pacific SST, and d) tropical east Pacific SST

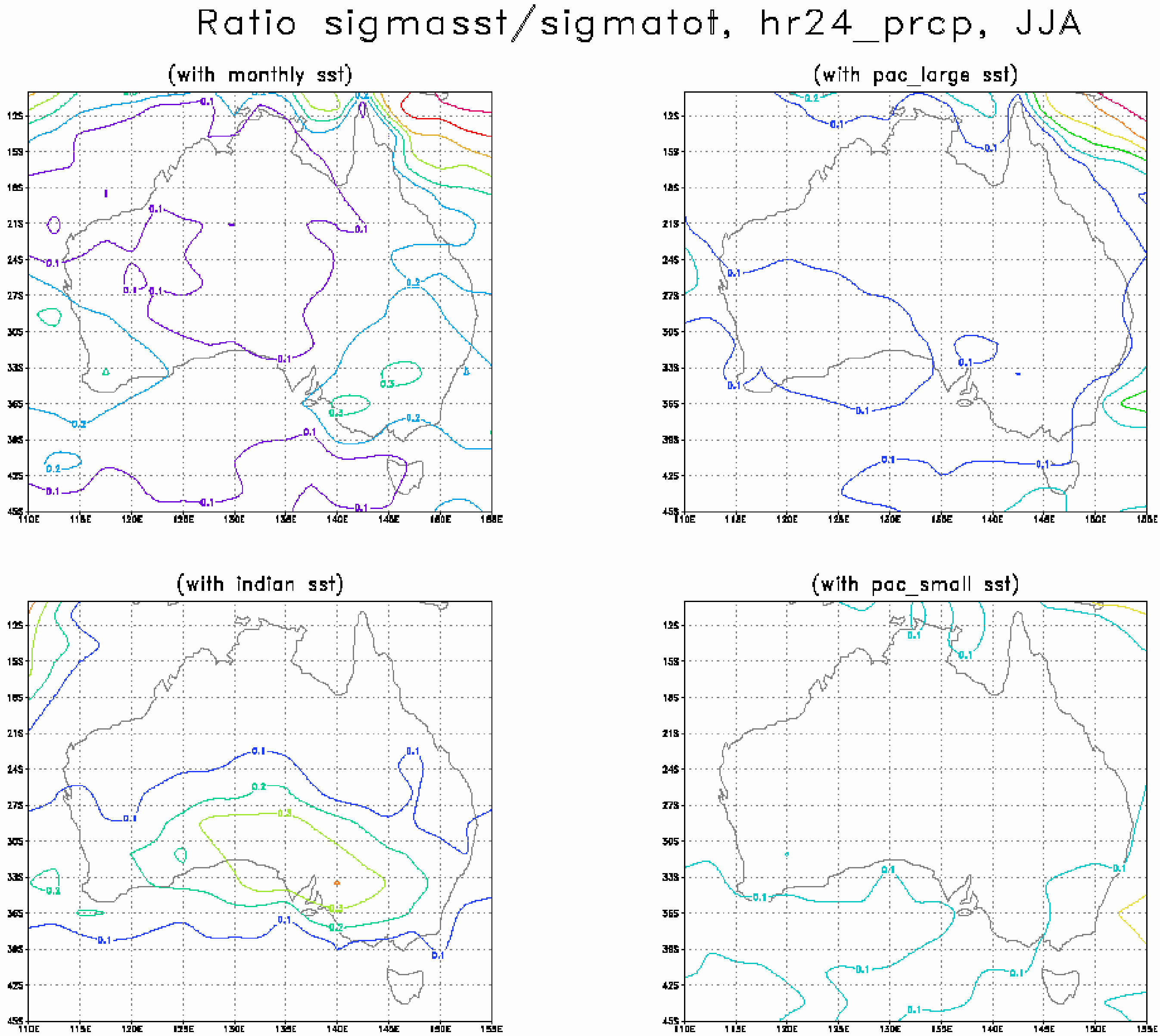

Figure 4. Predictable fraction of winter time rainfall variability forced by a) global SST, b) Indian Ocean SST, c) tropical Pacific SST, and d) tropical east Pacific SST

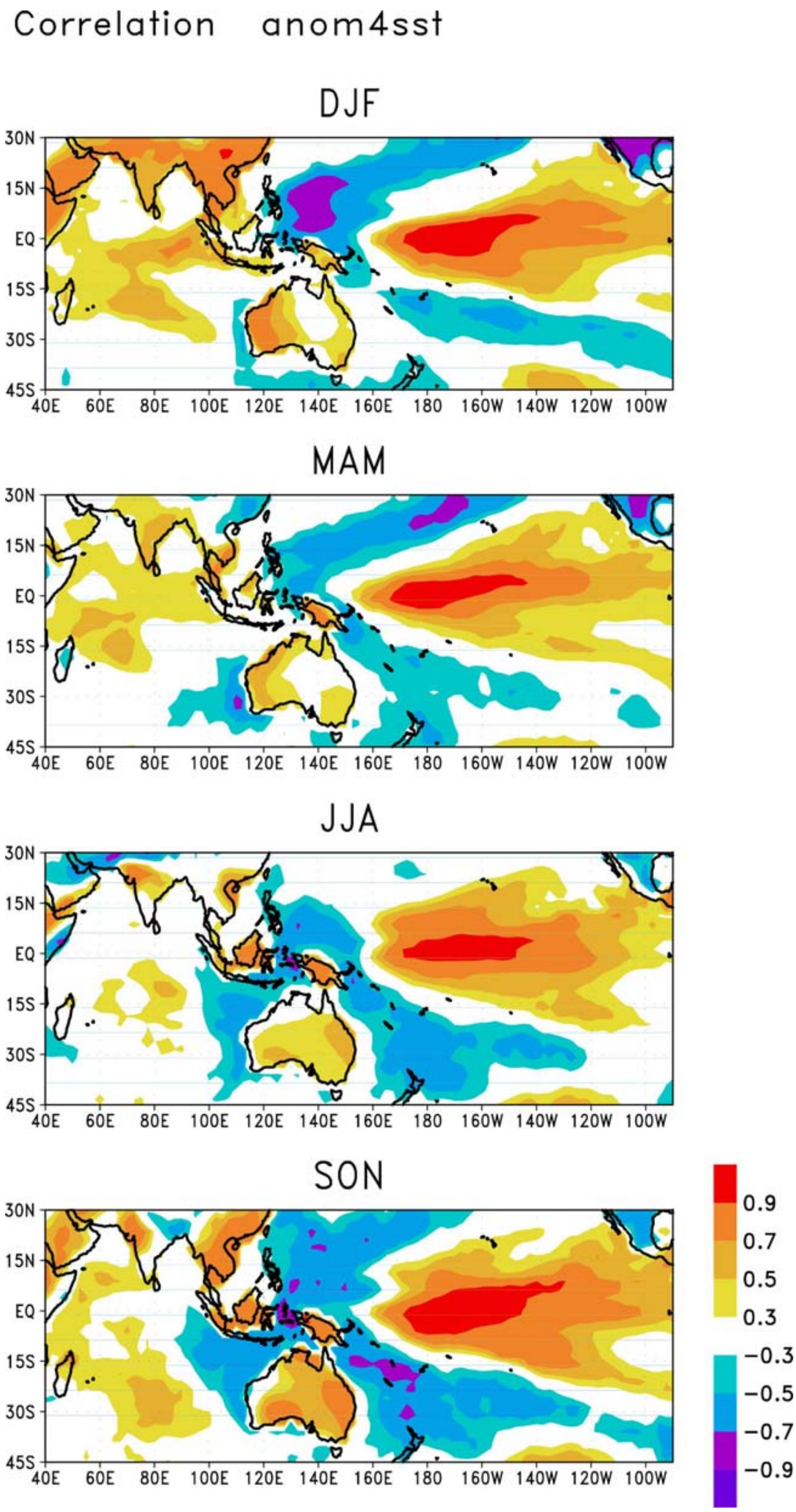

Figure 5. Correlation of Indo-Pacific SST with the Nino4 SST index by season

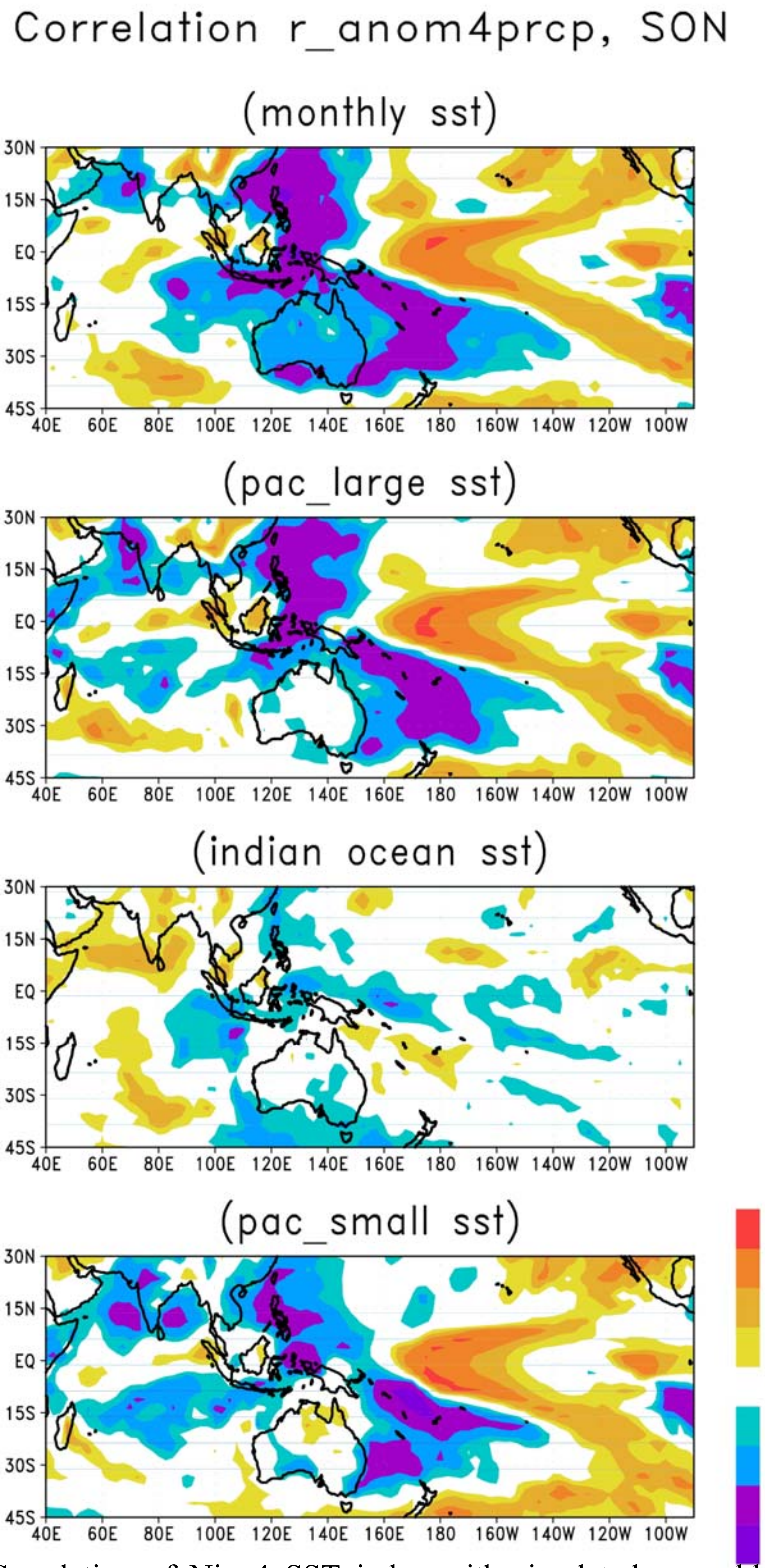

Figure 6. Correlation of Nino4 SST index with simulated ensemble mean rainfall SON

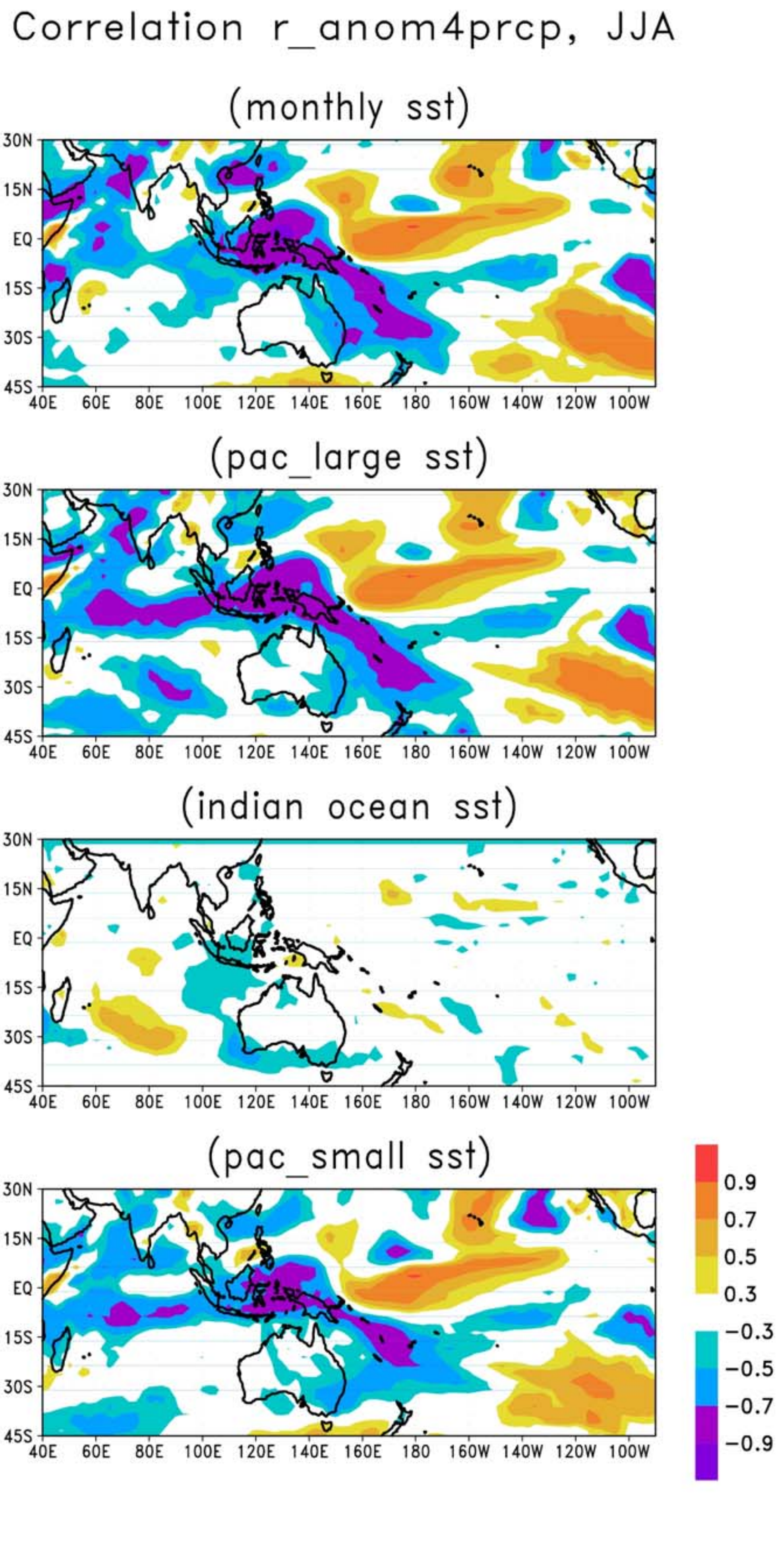

Figure 7 Correlation of Nino4 SST index with simulated ensemble mean rainfall for JJA.

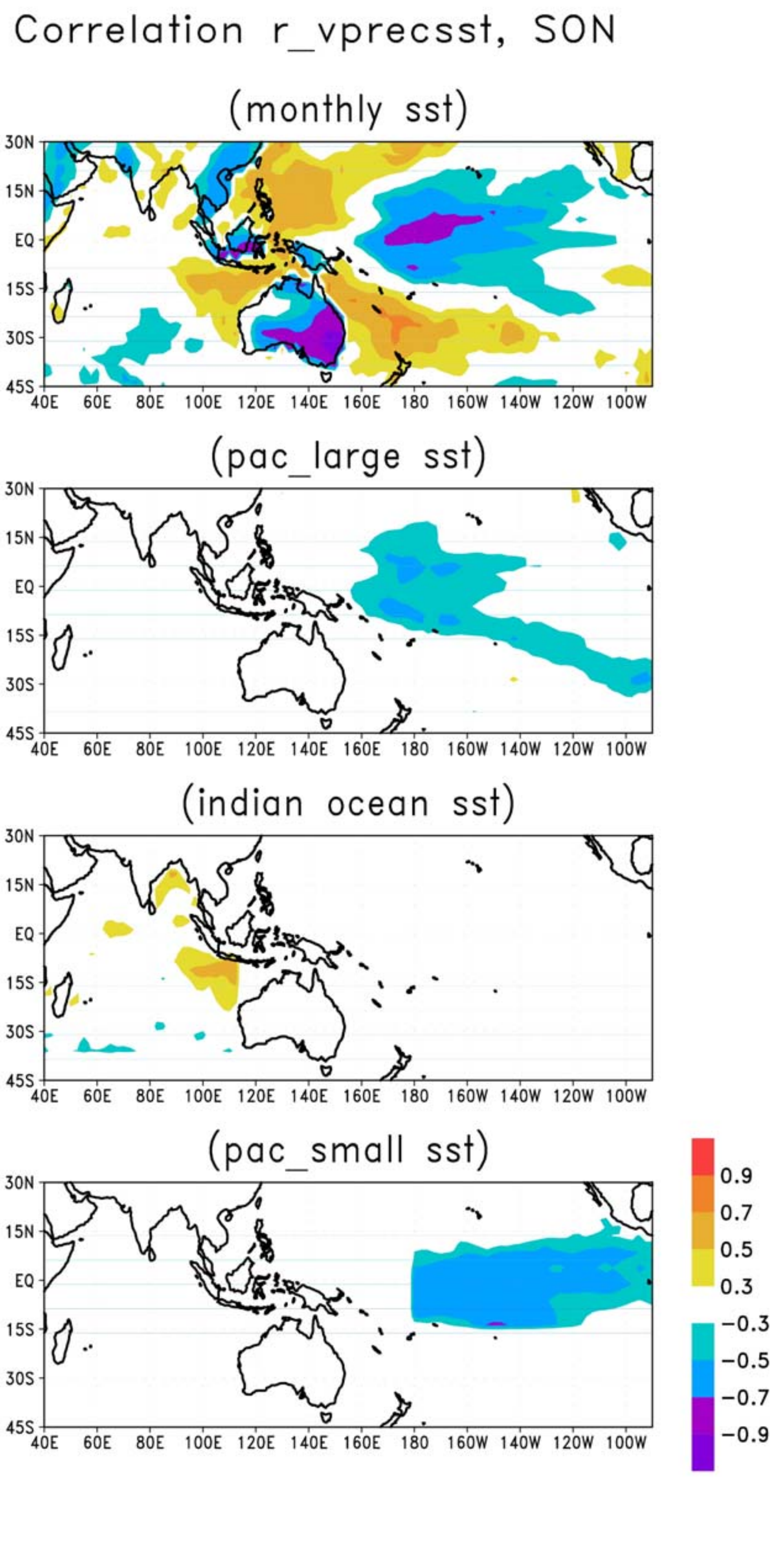

Figure 8. Correlation of SE Australian-mean rainfall with SST in the four experiments for the SON season.